Journal of the Marine Biological Association of the United Kingdom, 2015, 95(5), 1025–1031.
doi:10.1017/S0025315415000119

Does the tunic nipple array serve to camouflage diurnal salps?

EUICHI HIROSE[1], DAISUKE SAKAI[2], TOMOHIRO SHIBATA[3], JUNJI NISHII[3], HIROYUKI MAYAMA[4], AKIHIRO MIYAUCHI[5] AND JUN NISHIKAWA[6]

[1]Faculty of Science, University of the Ryukyus, Nishihara, Okinawa 903-0213, Japan, [2]Department of Electrical and Electronic Engineering, Kitami Institute of Technology, 165 Koen-cho, Kitami, Hokkaido 090-8507, Japan, [3]Research Institute for Electronic Science, Hokkaido University, Kitaku, Sapporo, Hokkaido 001-0020, Japan, [4]Department of Chemistry, Asahikawa Medical University, Midorigaoka-Higashi, Asahikawa 078-8510, Japan, [5]Hitachi Research Laboratory, Hitachi Ltd., Omika, Hitachi, Ibaraki 319-1292, Japan, [6]Department of Marine Biology, School of Marine Science and Technology, Tokai University, 3-20-1, Orido, Shimizu, Shizuoka 424-8610, Japan

The salp Thalia rhomboides *is distributed in the shallow depths during the day, and is thus at increased risk of predation by visual predators and from the damaging effects of ultraviolet (UV) radiation compared with species distributed in deeper layers in the daytime. The integument (tunic) of* T. rhomboides *may have adaptive optical properties, but the absorption spectra of the unfixed tunic demonstrate that the tunic transmits UV as well as visible light, indicating that the tunic is not an effective barrier against UV radiation. Ultrastructural observation revealed that the surface of the tunic cuticle is covered in a nipple array consisting of hemispherical protuberances approximately 40 and 30 nm in diameter in solitary and aggregate zooids, respectively. Simulation of light reflection of a nipple array using rigorous coupled wave analysis (RCWA) indicated that the reflection is slightly lower for the nipple array than for a flat surface at high angles of incidence ($\theta > 80^{\circ}$). This result supports the idea that the nipple array serves to make the salp less visible. The simulation also indicated that the height and distribution of the salp nipple array do not have an optimal structure for causing an antireflection effect. A mechanical restriction might exist on the structures, and the nipple array could also serve another function. The size and distribution of nipples may be controlled by the need to meet the complex requirements of multiple essential functions.*

Keywords: antireflection, nipple array, rigorous coupled wave analysis (RCWA), tunic cuticle, ultrastructure, UV

Submitted 31 May 2014; accepted 30 January 2015; first published online 17 March 2015

INTRODUCTION

Salps are gelatinous zooplankton with bodies that are essentially transparent. These organisms lack hard tissues and attack organs to protect their body, and thus transparency is important for the avoidance of visual predators. Diel vertical migration (DVM) is a well-known behaviour in some salps such as *Salpa* spp. These organisms occupy relatively deep (i.e. darker) layers of the water column during the day and come up to shallow depths at night (e.g. Madin *et al.*, 1996; Nishikawa & Tsuda, 2001). In contrast, others, including *Thalia*, are active in the shallow water layers throughout the day and are exposed to sunlight (Gibbons, 1997). Invisibility would therefore be more crucial for the survival of these non-migrating salps. Ultraviolet (UV) radiation that penetrates the water column is another harmful risk factor for pelagic organisms in shallow water, particularly in tropical–subtropical areas because of the high transparency of water and the low angle of incidence of solar radiation.

Some invertebrates have an array of submicron-scale protuberances on their body surfaces. For example, the surface of the compound eyes of moths is covered with cuticular protuberances known as the corneal nipple array, which reduces eye glare by forming a refractive index gradient (e.g. Bernhard, 1967; Stavenga *et al.*, 2006). This antireflection property (the 'moth-eye effect') is effective for decreasing visibility to predators. Similar nipple arrays have been described in some aquatic invertebrates such as annelids (Hausen, 2005), entoprocts (Nielsen & Jespersen, 1997; Iseto & Hirose, 2010), echinoderms (Holland, 1984), and ascidians (Hirose *et al.*, 1997). However, whether the nipple array also serves a cryptic function in the aquatic benthos is unknown (Johnsen, 2003).

The body of salps is entirely covered with a transparent, gelatinous tunic that consists of an extracellular matrix overlying the epidermis. Although the tunic is a fibrous matrix composed primarily of cellulose (Hirose *et al.*, 1999), the tunic surface is covered with an electron-dense layer of cuticle that would protect the tunic from the invasion of microorganisms. Some salp species, such as *Thetys vagina*, have an array of cuticular protrusions $\leq$50 nm in height (Hirose *et al.*, 1999). To better understand the optical properties of the salp tunic, we studied the fine surface structures of the tunic of the diurnal salp *Thalia rhomboides* and measured the absorption spectra of the transparent tunic. The presence of the moth-eye effect was tested underwater using a nanopillar sheet as a model for the nipple array. In addition, we simulated the reflectance of incident light on nipple arrays of various sizes and distributions.

Corresponding author:
E. Hirose
Email: euichi@sci.u-ryukyu.ac.jp

MATERIALS AND METHODS

Animals

Solitary and aggregate individuals of *T. rhomboides* were collected from several net tows near Sesoko Island (Okinawa, Japan). Intact animals were sorted at Sesoko Station (Tropical Biosphere Research Center, University of the Ryukyus), and the live specimens were brought to the laboratory. Although the salp individuals are almost transparent under transmitted light illumination aside from their alimentary tracts, the transparent tunic is visible under oblique illumination (Figure 1).

Measurement of absorption spectra

The tunic of *T. rhomboides* was cut into a rectangular sheet (5–10 mm per side) with scissors and razor blades. Individual sheets of live tunic material were attached to the wall of a quartz cell, and the 280–800-nm absorption spectra were recorded at 1-nm intervals with a UV-1650PC spectrophotometer (Shimadzu, Otsu, Shiga, Japan). For an example of a tunic containing UV-absorbing substances, we referred to the absorption spectra of *Diplosoma virens* (a colonial ascidian-associated cyanobacteria) from our previous study (Hirose *et al.*, 2004).

Microscopy

Tunic sheets were fixed with 2.5% glutaraldehyde in a 0.45 M sucrose and 0.1 M cacodylate buffer (pH 7.5) at 4°C for 2 h. The specimens were briefly rinsed with the same buffer, post-fixed with 1% osmium tetroxide in a 0.1 M cacodylate buffer (pH 7.5) at 4°C for 1.5 h, and then dehydrated through an ethanol series. The specimens were embedded in an epoxy resin for transmission electron microscopy (TEM). Sections were stained with uranyl acetate and lead citrate and examined under a transmission electron microscope (JEM-1011; JEOL, Tokyo, Japan) at 80 kV. For scanning electron microscopy (SEM), specimens were dehydrated through an ethanol series, immersed in *t*-butanol and freeze-dried, sputter-coated with gold-palladium, and examined under a scanning electron microscope (JSM-6060LV; JEOL) at 15 kV.

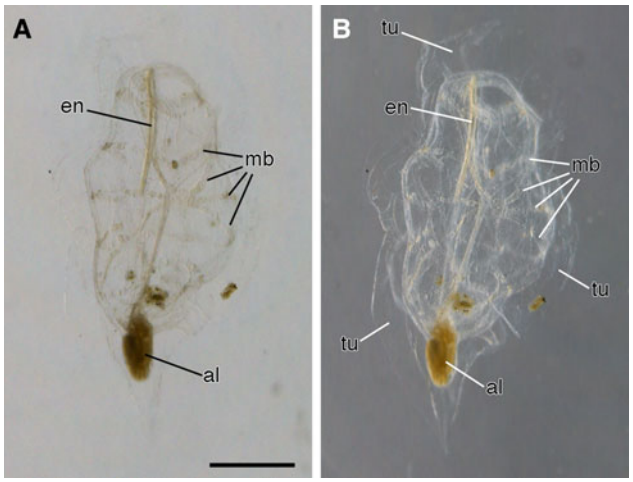

Fig. 1. An individual of *Thalia rhomboides*, aggregate zooid (fixed specimen). The tunic is nearly invisible under transmitted light (A) but visible under oblique illumination (B). al, alimentary tract; en, endostyle; mb, muscle band; tu, tunic. Scale bar = 1 mm.

Light reflection of the nanopillar sheet underwater

Polystyrene nanopillar sheets (20 × 20 mm) were hydrophilized by oxygen plasma etching: each sheet has a flat surface or arrays of 1 μm-high nanopillars 0.5 or 2 μm in diameter (Kuwabara & Miyauchi, 2008). Each sheet has either a flat surface or arrays of 1 μm high nanopillars 0.5 or 2 μm in diameter. The sheets with or without nanopillars were fixed side by side to a plastic board. The light reflected on the sheets from a fluorescent tube was photographed both in and out of water.

Simulation of light reflection of a nipple array

We calculated the light reflection at the border between the medium (seawater) and matrix (tunic) with or without the nipple array with rigorous coupled wave analysis (RCWA) using DiffractMOD3.2 software (RSoft Design Group, Inc., Ossining, NY, USA). The light reflectance on the flat surface will be larger when the difference of refractive indices is larger between the medium and material. The refractive index of the medium (seawater) was 1.343 in the simulation. The exact refractive index of the tunic is unknown. Since the water content of tunic is so high, the refractive index would not differ much from that of seawater. Therefore, we assumed the refractive index of the matrix (tunic) to be 1.443. Polarized lights were used for this simulation, both transverse electric wave (TE wave) and transverse magnetic wave (TM wave). For the salp nipple array model, based on our electron microscope observations of the salp tunic, we assumed that each nipple consisted of a hemisphere and column 80 nm in diameter (Figure 2). The nipples were distributed evenly. Parameters for the simulation included the following: wavelength of light (λ: 200–700 nm), angle of incidence of light (θ: 10–90°), height of the nipple (h: 0–400 nm), and distance between the apices of adjacent nipples (d: 80–10 μm). Nipple arrays have a specific optical effect on the light reflection, when the optical path length is close to the wavelength. Here, the optical path length is the product of the difference of refractive indices and the pillar height. In the range of the present simulation, the optical effect of the nipple arrays is proportional to the difference of the refractive indices, since the optical path length (0–40 nm) is much shorter than the wavelength (200–700 nm).

RESULTS

Absorption spectra of the tunic

For *T. rhomboides* individuals of both aggregate and solitary zooids, the absorption spectra of the tunic showed no specific absorption peaks in the range of visible light (400–760 nm), UV-A (325–400 nm) or UV-B (280–315 nm) (black lines in Figure 3). In contrast, the absorption spectra of the tunic containing UV-absorbing substances displayed a prominent absorption peak at around 320 nm (grey line in Figure 3).

https://doi.org/10.1017/S0025315415000119 Published online by Cambridge University Press

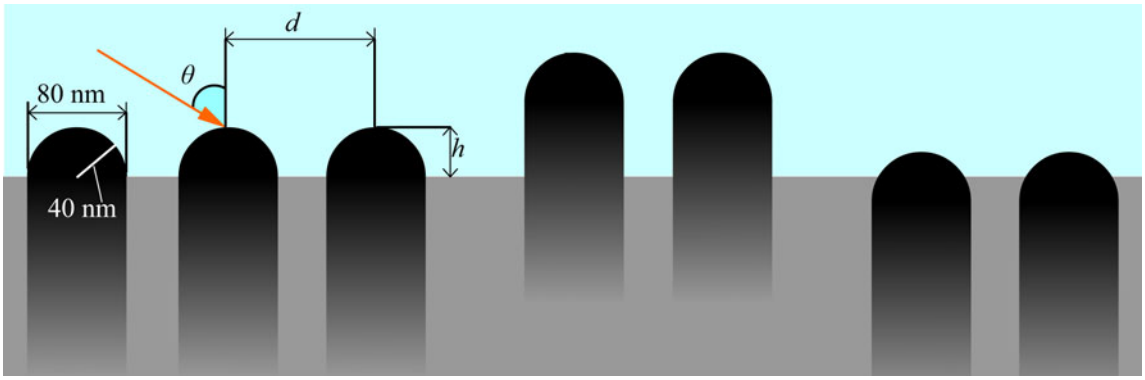

Fig. 2. A model of the nipple array and the parameters for the simulation of light reflection. Each nipple consists of a hemisphere and column 80 nm in diameter. Standard model (left) is 40 nm high, with taller nipples (middle) and shorter nipples (right) shown for comparison. *d*, distance between nipple apices; *h*, nipple height; *θ*, angle of incidence of light.

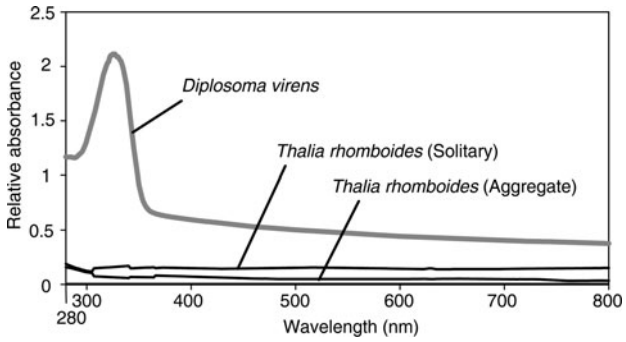

Fig. 3. Absorption spectra of the tunic of *Thalia rhomboides* (black lines) and the tunic of the colonial ascidian *Diplosoma virens* that harbours the algal symbiont *Prochloron* (grey line). The spectra of *D. virens* have an absorption peak due to UV-absorbing substances, whereas the spectra of *T. rhomboides* have no prominent peak.

Fine structures of the tunic surface

The tunic of solitary individuals of *T. rhomboides* had a thin cuticular layer approximately 25 nm thick, and the cuticle was lined with an electron-dense subcuticle layer of 200 nm thickness (Figure 4A). Numerous minute protuberances densely cover the cuticle layer. Under SEM, the protuberances were distributed at roughly even intervals and formed an array of nipples (Figure 4B). The average height of the protuberances was 40.5 nm (SD = 6.18, N = 21), the diameter at the base was 77.3 nm (SD = 8.64, N = 21), and the spacing between the apices of the protuberances was 100 nm (SD = 15.2, N = 16).

The ultrastructures of the tunics of aggregate individuals were essentially the same as those of solitary individuals, but the cuticle was not lined with a subcuticle layer (Figure 4C, D). The minute protuberances were shorter, and the spacing between the protuberances was greater than those in solitary individuals. As shown in Figure 4C, D, the spacing between the protuberances differed among sections from the same individual. The average height of the protuberances was 31.5 nm (SD = 5.77, N = 13), the diameter at the base was 59.0 nm (SD = 15.9, N = 13), and the distance between the apices was 112 nm (SD = 22.1, N = 9).

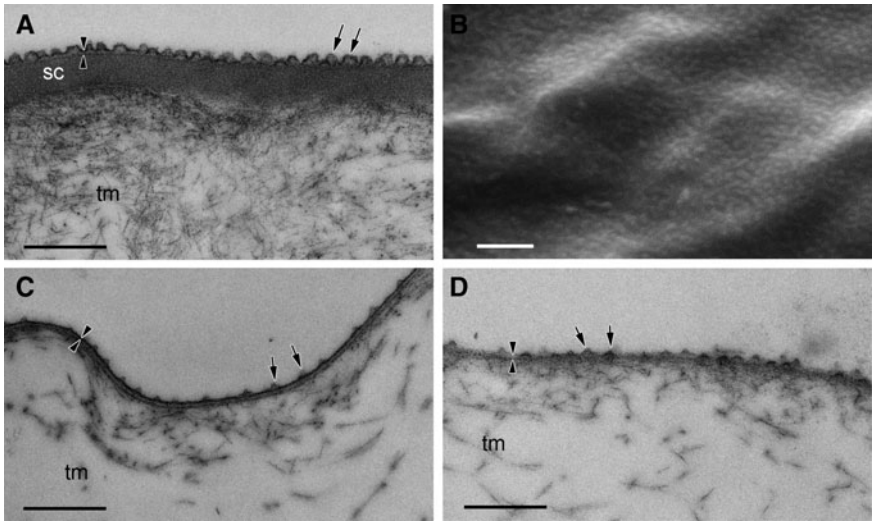

Fig. 4. TEM (A, C, D) and SEM (B) micrographs of the tunic cuticle of *Thalia rhomboides* for solitary (A, B) and aggregate zooids (C, D). Fibrous tunic matrix (tm) is covered with an electron-dense layer of tunic cuticle (arrowheads). Minute protuberances occur on the tunic surface (arrows). Electron-dense subcuticle layer (sc) lies beneath the cuticle in the tunic of the solitary specimen. Scale bars = 0.5 μm.

https://doi.org/10.1017/S0025315415000119 Published online by Cambridge University Press

Light reflection of the nanopillar sheets

Light reflection of the pillared surface was less than of the flat surface in air (Figure 5A). Reduced light reflection was also observed for the pillared surface underwater, although the light intensity was greatly reduced by the reflectivity of the water surface (Figure 5B). Less reflection occurred for the sheet with the 0.5 μm diameter pillars than the sheet with the 2 μm diameter pillars both in air and underwater. SEM images of the sheets with and without pillars are shown in Figure 5C.

Simulation of light reflection

Based on the tunic cuticle protuberances of solitary individuals of *T. rhomboides* (see above), we configured the standard model of the nipple array with 80 nm diameter hemispheres evenly spaced 100 nm apart between the apices: i.e. $h = 40$ nm and $d = 100$ nm (see Figure 2, left).

Similar properties of light reflection versus angle of incidence were observed for the 200–700 nm wavelengths in the standard model: the reflectance increased with increased angle of incidence (θ), with maximum reflection at 90° (see online Supplementary Figure S1). The reflectance was low when the angle of incidence was low, and the reflectance was less than 2% when the angle of incidence was less than 70°. The angle of incidence for the 10% reflectance was 78.6 and 76.3° for TM and TE waves, respectively, for a light wavelength of 633 nm.

The height of the nipple (h) and the angle of incidence drastically changed the reflectance. Figure 6 shows the relative reflectance of the nipples (20–400 nm height) compared with the reflectance of the flat surface ($h = 0$) for angles of incidence from 60 to 89°. The wavelength was 633 nm and the spacing of the nipples was 100 nm in this simulation. Although the curve of the relative reflectance–angle of incidence did not simply rise to the right (Figure 6), the relative reflectance decreased with increased nipple height at high angles of incidence ($\theta > 80°$). The spacing of the nipples (d) also changed the reflectance, and the relative reflectance compared with the reflectance of the flat surface was a minimum of 100–250 nm in the present simulation ($\theta = 75°$, $\lambda = 633$ nm, $h = 20$–400 nm) (Figure 7). The optimal distances and heights for antireflection are shown in Figure 8; the optimal distance increased with nipple height.

DISCUSSION

The tunic of *T. rhomboides* is almost transparent in the range of visible light (400–760 nm), UV-A (325–400 nm) and UV-B (280–315 nm), indicating that the tunic does not contain compounds for UV protection. This is consistent with the image of the salp observed under transmitted light illumination. Although ultrastructural observation revealed the presence of a nipple array on the tunic surface, the reflection of UV light did not differ from that of visible light in the simulation of the standard nipple array model mimicking the salp tunic. Therefore, the nipple array on the salp tunic is not important for UV protection. UV light is rarely attenuated in the tunic and passes through the internal tissues of the salps during the day; therefore, UV radiation should be harmful for non-migrating salps such as *T. rhomboides* that inhabit shallow zones in tropical–subtropical waters. Nonetheless,

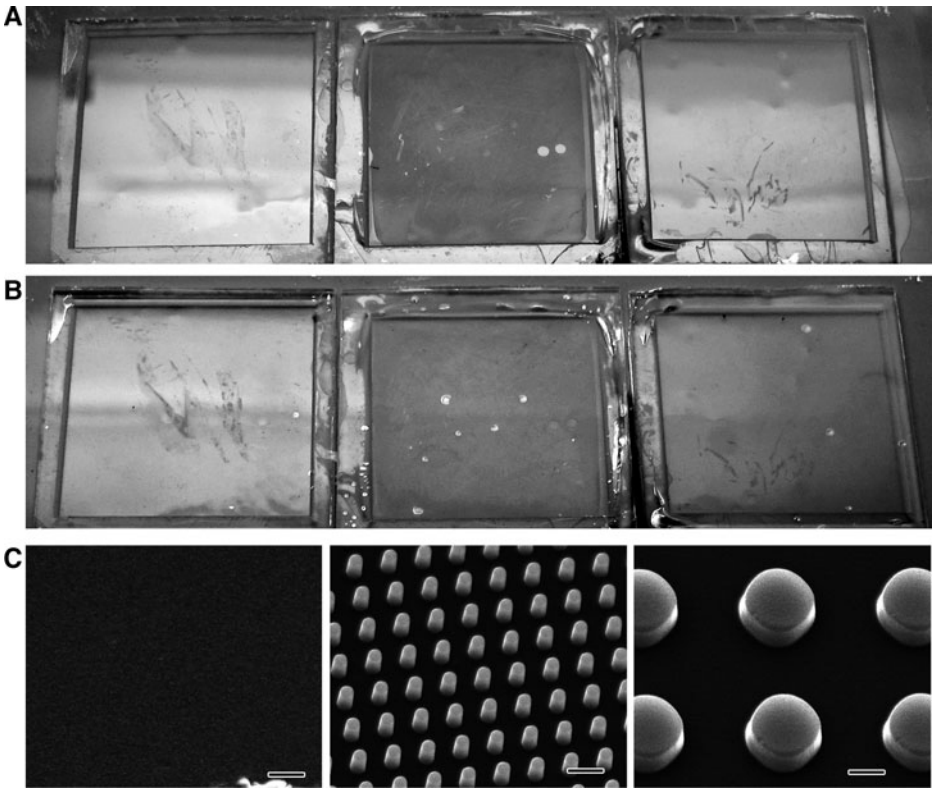

Fig. 5. Light reflection (A, in air; B, underwater) and SEM images (C) of the polystyrene sheets with 2 μm diameter pillars (right), 0.5 μm diameter pillars (middle) and no pillars (i.e. flat sheet) (left). Scale bars in C indicate 1 μm.

https://doi.org/10.1017/S0025315415000119 Published online by Cambridge University Press

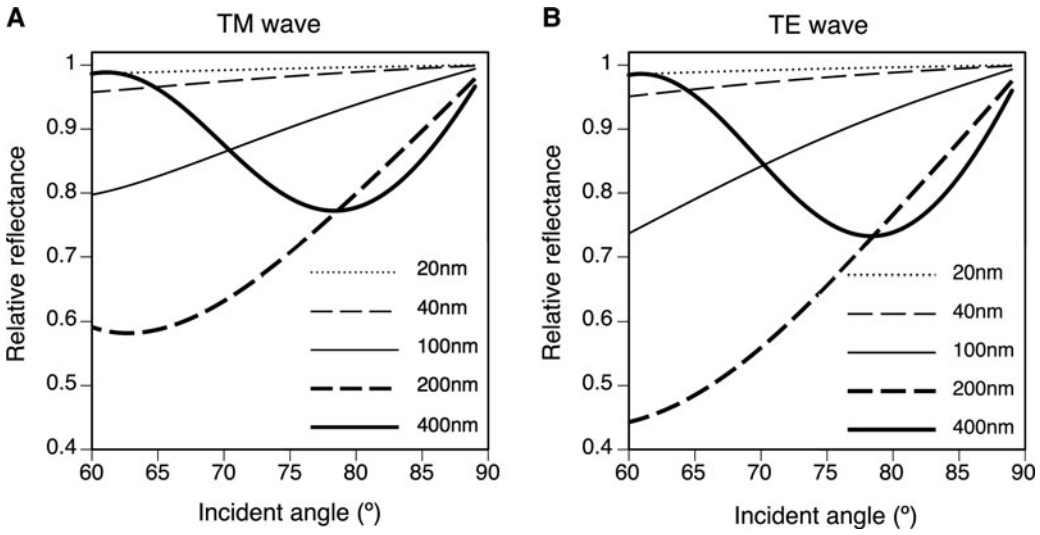

Fig. 6. Relative reflectance compared with the reflectance of the flat surface ($h = 0$) for various nipple array heights ($h = 20$, 40, 100, 200 and 400 nm) for an angle of incidence (θ) range from 60 to 89°. $\lambda = 633$ nm, $d = 100$ nm. (A) TM wave. (B) TE wave.

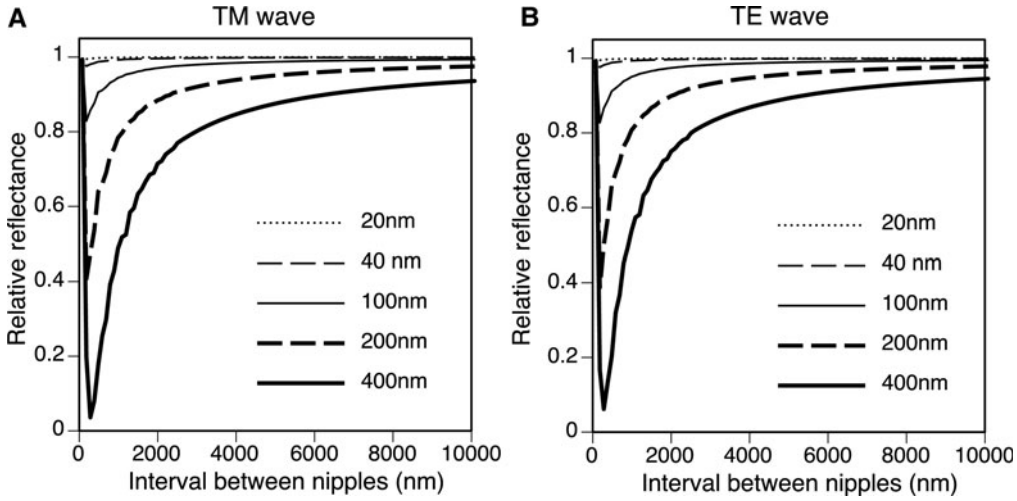

Fig. 7. Relative reflectance compared with the reflectance of the flat surface ($h = 0$) for nipple spacing (d) from 80 nm to 10 μm. $\theta = 75°$, $\lambda = 633$ nm. (A) TM wave. (B) TE wave.

transparency for predator avoidance may be more crucial for the salps than UV protection. Muscle and/or alimentary tract occasionally look blue in some *Thalia* individuals, whereas these tissues are not always blue in the same species. The blue tissues are possibly an adaptation to UV light, considering the small contribution of the tunic to the UV protection.

Light reflection of the polystyrene nanopillar sheet was smaller than that of the flat surface in both air and water, indicating that the nipple array is effective for antireflection in an aquatic environment. The salp tunic rarely reflected light in the simulation of the standard model based on the tunic cuticle ultrastructures (hemispheres 80 nm in diameter at 100 nm intervals), except for light at high angles of incidence. This is consistent with our experience in the field; the outline of the transparent tunic is visible under oblique illumination, and reflected light is prominent when the background is dark. This condition is known as dark-field illumination, and reduction of the reflections of the light at high angles will decrease the visibility. As light scattering is a major factor undermining the camouflage transparency of zooplankton (Gagnon *et al.*, 2007), the antireflection properties of the tunic surface would be important for salps active in shallow depths during the day. Kashkina (1986) lists 47 species of fish in 10 orders that are known to feed on salps, indicating the visual predators are natural enemies of salps.

In the simulations using rigorous coupled wave analysis, we assumed the refractive index of the tunic to be 1.443, because the water content of the tunic is so high that the refractive index would not differ much from that of seawater (1.343). The light reflection depends on the difference of refractive indices between the medium (seawater) and the material (tunic) on the flat surface. Thus the real reflection will be smaller, if the real refractive index of the tunic is smaller than our estimate. Nipple arrays have a specific optical effect on the light reflection, when the optical path length is close to the wavelength. However, the optical path length (0–40 nm) is much shorter than the wavelength (200–700 nm) in the range of the present simulation.

https://doi.org/10.1017/S0025315415000119 Published online by Cambridge University Press

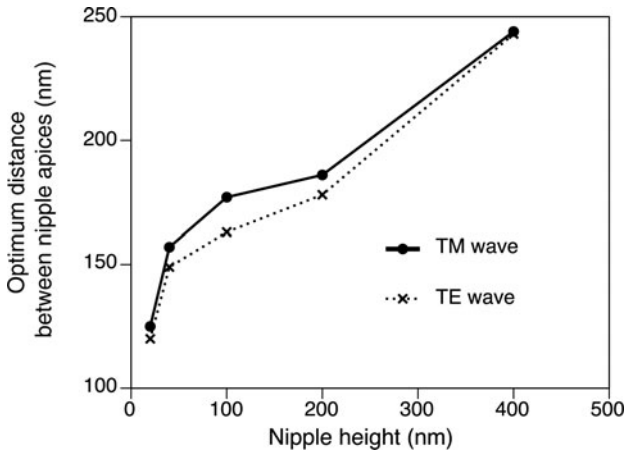

Fig. 8. The optimal distribution for nipple array antireflection ($h = 20$–400 nm) for TM wave (solid line) and TE wave (dotted line). $\theta = 75°$, $\lambda =$ 633 nm.

Accordingly, the relative changes of reflectance against variables (e.g. wavelength, incident angle and pillar height) are proportional to the difference between the refractive indices, resulting in similar curves. Therefore, the simulation with the hypothetical refractive index for the tunic is useful to discuss the optical property of nipple arrays.

Thalia rhomboides nipple height was about 40 nm for solitary individuals and about 30 nm for aggregate individuals, whereas the height of nipples in ascidians ranges from 20 to 150 nm (Hirose *et al.*, 1997). Stavenga *et al.* (2006) calculated the reflectance of three nipple array types. Cone, paraboloid and Gaussian-shaped nipples served as mimetic models of the moth-eye corneal nipple array using a multilayer model, showing that reflectance decreases with increasing nipple height. Similar results were obtained from our simulations with a hemisphere and column model using RCWA: the relative reflectance decreased with increased nipple height at high angles of incidence ($\theta > 80°$). Although the curve for the relationship between the relative reflectance and the angle of incidence does not simply rise to the right for lower angles of incidence (Figure 6), light reflection for low angles of incidence is very small and is negligible for the antireflection function (see online Supplementary Figure S1). The relative reflectance to the reflectance of the flat surface was always less than 1 on the nipple arrays at high angles of incidence ($>80°$), indicating that the nipple arrays are effective for the reduction of visibility (Figure 6). In our simulation, higher nipple reduces more at high angle, and hence, the real nipple on the salp (~40 nm in height) was not optimal in size for antireflection. The reflectance also depends on the spacing between the nipples. For antireflection, the optimal distribution is estimated to be about 150 nm for salps with 40 nm high nipples, although the actual spacing is about 100 nm. Therefore, the salp nipple array is not structurally optimal for the antireflection effect. Why salps do not have taller nipples with greater spacing to decrease reflection more effectively is unknown, although the thin tunic layer may lack sufficient strength to support a larger nipple array. In addition, the salp nipple array may serve another function. For example, a hydrophilic nipple array has a bubble-repellent property in water (Hirose *et al.*, 2013). Because the attachment of bubbles would be a serious problem for plankton, causing unfavourable buoyancy, this may be an important function of the salp nipple array. If the nipple array is a multifunctional structure, the size and distribution of the nipples may be controlled by the need to meet the complex requirements of essential functions.

ACKNOWLEDGEMENTS

This study is supported by the Interdisciplinary Collaborative Research Programme of the Atmosphere and Ocean Research Institute, the University of Tokyo. We thank Shohei Kadena and Yoshikatsu Nakano (Tropical Biosphere Research Center, University of the Ryukyus) for supporting material collection.

SUPPLEMENTARY MATERIALS AND METHODS

The supplementary material referred to in this paper can be found online at journals.cambridge.org/mbi.

REFERENCES

Bernhard C.G. (1967) Structural and functional adaptation in a visual system. *Endeavour* 26, 79–84.

Gagnon Y.L., Shashar N., Warrant E.J. and Johnsen S.J. (2007) Light scattering by selected zooplankton from the Gulf of Aqaba. *Journal of Experimental Biology* 210, 3728–3735.

Gibbons M.J. (1997) Vertical distribution and feeding of *Thalia democratica* on the Agulhas Bank during March 1994. *Journal of the Marine Biological Association of the United Kingdom* 77, 493–505.

Hausen H. (2005) Comparative structure of the epidermis in polychaetes (Annelida). *Hydrobiologia* 535/536, 25–35.

Hirose E., Kimura S., Itoh T. and Nishikawa J. (1999) Tunic morphology and cellulosic components of pyrosomas, doliolids, and salps (Thaliacea, Urochordata). *Biological Bulletin* 196, 113–120.

Hirose E., Lambert G., Kusakabe T. and Nishikawa T. (1997) Tunic cuticular protrusions in ascidians (Chordata, Tunicata): a perspective of their character-state distribution. *Zoological Science* 14, 683–689.

Hirose E., Mayama H. and Miyauchi A. (2013) Does the aquatic invertebrate nipple array prevent bubble adhesion? An experiment using nanopillar sheets. *Biology Letters* 9, 20130552.

Hirose E., Ohtsuka K., Ishikura M. and Maruyama T. (2004) Ultraviolet absorption in ascidian tunic and ascidian-*Prochloron* symbiosis. *Journal of the Marine Biological Association of the United Kingdom* 84, 789–794.

Holland N.D. (1984) Echinodermata: epidermal cells. In Bereiter-Hahn J., Matoltsy A.G. and Richards K.S. (eds) *Biology of the integument, 1. Invertebrates*. Berlin: Springer, pp. 756–774.

Iseto T. and Hirose E. (2010) Comparative morphology of the foot structure of four genera of Loxosomatidae (Entoprocta): implications for foot functions and taxonomy. *Journal of Morphology* 271, 1185–1196.

Johnsen S. (2003) Lifting the cloak of invisibility: the effect of changing optical conditions on pelagic crypsis. *Integrative and Comparative Biology* 43, 580–590.

Kashkina A.A. (1986) Feeding of fishes on salps (Tunicata: Thaliacea). *Journal of Ichthyology* 26, 57–64.

https://doi.org/10.1017/S0025315415000119 Published online by Cambridge University Press

Kuwabara K. and Miyauchi A. (2008) High-aspect-ratio nanopillar structures fabricated by nanoimprinting with elongation phenomenon. *Journal of Vacuum Science & Technology B* 8, 582–584.

Madin L.P., Kremer P. and Hacker S. (1996) Distribution and vertical migration of salps (Tunicata, Thaliacea) near Bermuda. *Journal of Plankton Research* 18, 747–755.

Nielsen C. and Jespersen A. (1997) Entoprocta. In Harrison F.W. and Woollacott R.M. (eds) *Microscopic anatomy of invertebrates*, Volume 13. New York, NY: Wiley, pp. 13–43.

Nishikawa J. and Tsuda A. (2001) Diel vertical migration of the pelagic tunicate, *Salpa thompsoni* in the Southern Ocean during the austral summer. *Polar Biology* 24, 299–302.

and

Stavenga D.G., Foletti S., Palasantzas G. and Arikawa K. (2006) Light on the moth-eye corneal nipple array of butterflies. *Proceedings of the Royal Society B* 273, 661–667.

Correspondence should be addressed to:
E. Hirose
Faculty of Science, University of the Ryukyus,
Nishihara, Okinawa 903-0213,
Japan
email: euichi@sci.u-ryukyu.ac.jp

https://doi.org/10.1017/S0025315415000119 Published online by Cambridge University Press